



A search for associated production of a b quark and a neutral Higgs boson which decays to taus in supersymmetric models

The DØ Collaboration

URL <http://www-d0.fnal.gov>

(Dated: August 13, 2009)

We report results from a search for production of a neutral Higgs boson in association with a b quark. We look for Higgs decays to tau pairs with one tau subsequently decaying to a muon and the other to hadrons. The data come from 2.7 fb^{-1} of $p\bar{p}$ collisions recorded by the DØ detector at $\sqrt{s} = 1.96 \text{ TeV}$. The data are found to be consistent with background predictions. The result is used to exclude a region of parameter space of the minimal supersymmetric model.

Preliminary Results for Summer 2009 Conferences

The current model of nature at high energies, the standard model (SM), has withstood increasingly precise experimental tests, although the Higgs boson needed to mediate the breaking of electroweak symmetry has not been found. Despite the success of the SM, it has several shortcomings. Theories invoking a new fermion-boson symmetry, called supersymmetry [1] (SUSY), provide an attractive means to address some of these including the hierarchy problem and nonunification of couplings at high energy. In addition to new SUSY-specific partners to SM particles, these theories have an extended Higgs sector. Minimal SUSY models have two Higgs doublet fields which result in five Higgs bosons: two neutral scalars (h^0, H^0), a neutral pseudoscalar (A^0) and two charged Higgs bosons (H^\pm). The mass spectrum of the Higgs bosons can be determined at tree level by two parameters, but at higher order additional parameters are needed. The tree level parameters are typically chosen to be $\tan\beta$, the ratio of the vacuum expectation values of up-type and down-type scalar fields and M_A , the mass of the physical pseudoscalar. Higher order corrections are dominated by the Higgsino mass parameter μ and the mixing of scalar top quarks.

In this Letter, we present a search for neutral Higgs bosons (collectively denoted ϕ) produced in association with a b quark. The specific Higgs boson decay mode used in this search is $\phi \rightarrow \tau\tau$ with one of the taus subsequently decaying via $\tau \rightarrow \mu\nu_\tau\bar{\nu}_\mu$ and the second via $\tau \rightarrow \text{hadrons} + \nu_\tau$ (denoted τ_h). In SUSY models the cross section is enhanced by a factor $\propto \tan^2\beta$ relative to the SM, giving potentially detectable rates. Two of the three neutral Higgs bosons have nearly degenerate masses over much of the parameter space, giving another factor of two in production rate. A previous search in this final state was carried out by the D0 experiment [2]. Searches in the related channels $\phi \rightarrow \tau\tau$ [3, 4] and $\phi b \rightarrow b\bar{b}\bar{b}$ [5, 6] have also been carried out by both the D0 and CDF experiments. This channel is complementary to the $\phi b \rightarrow b\bar{b}\bar{b}$ and $\phi \rightarrow \tau\tau$ channels. It has less sensitivity to SUSY radiative corrections than the $b\bar{b}\bar{b}$ final state, and the background prediction is less affected by $Z \rightarrow \tau\tau$ events than the $\phi \rightarrow \tau\tau$ process. The result presented in this Letter uses an integrated luminosity of 2.7 fb^{-1} which is eight times larger than that used for the previous result in this channel. Because of analysis improvements, the gain in sensitivity compared to the prior result is greater than expected from the increased integrated luminosity only.

The D0 detector [7] is a general purpose detector located at Fermilab's Tevatron $p\bar{p}$ collider. This analysis relies heavily on all aspects of the detector: tracking, calorimetry, muon detection, the ability to identify detached vertices and the luminosity measurement.

This search requires reconstruction of muons, hadronic tau decays, jets (arising from b quarks) and neutrinos. Muons are identified using track segments in the muon system and are required to have a track reconstructed in the inner tracking system which is close to the muon-system track segment in η and φ . Here η is the pseudorapidity and φ is the azimuthal angle in the plane perpendicular to the beam. Jets are reconstructed from calorimeter information using a midpoint algorithm [8] with a radius cutoff of $R = 0.5$ in (η, φ) space. Jets are additionally identified as being consistent with decay of a b -flavored hadron (b -tagged) if tracks aligned with the calorimeter jet have high impact parameter or form a vertex separated from the primary interaction point in the plane transverse to the beam as determined by a neural network (NN_b) algorithm [9]. Hadronic tau decays are identified [10] as jets in the calorimeter reconstructed [8] using cone radius $R = 0.3$ which have associated tracks. The tau candidates are then categorized as being one of three types which correspond roughly to one-prong tau decay with no π^0 s (called type 1), one-prong decay with π^0 s (type 2) and multiprong decay (type 3). A final identification requirement is placed on the output value of a neural network (NN) designed to separate taus from hadronic jets. The missing transverse energy \cancel{E}_T is used to infer the presence of neutrinos. The \cancel{E}_T is the negative of the vector sum of the transverse energy of all cells in the calorimeter satisfying $|\eta| < 3.2$. \cancel{E}_T is corrected for the energy scales of reconstructed final state objects.

Signal event acceptance and efficiency are modeled using simulated standard model ϕb events generated with the PYTHIA event generator [11] requiring the b quark to satisfy $p_T > 15 \text{ GeV}$ and $|\eta| < 2.5$ and using the CTEQ6L1 [12] parton distribution functions (PDF). The TAUOLA [13] program is used to model tau decay and EVTGEN [14] is used to decay b hadrons. The dependence of the Higgs boson decay width on $\tan\beta$ is included by reweighting PYTHIA samples. The generator outputs are passed through a detailed detector simulation based on GEANT [15]. Each GEANT event is combined with a collider data event recorded during a random beam crossing to account for instantaneous luminosity effects. The combined output is then passed to the D0 event reconstruction program. Simulated signal samples are generated for Higgs masses in the range 90 GeV to 210 GeV.

Backgrounds to this search are dominated by Z +jets events, $t\bar{t}$ events and multijet events (MJ). In the MJ background the apparent leptons result from misidentification of hadronic jets. Additional backgrounds include W +jets events, standard model diboson production and single top quark production. Except for the MJ contribution, all background yields are estimated using simulated events, with the same processing chain and correction factors used for signal events. The Z +jets, W +jets and $t\bar{t}$ samples are generated using ALPGEN [16] with PYTHIA used for fragmentation. The diboson samples are generated using PYTHIA. For simulated samples in which there is only one real lepton arising from the decay of a massive state, for example W +jets and $t\bar{t} \rightarrow \ell$ +jets, the second lepton is either a jet misidentified as a tau or a muon+jet system from heavy flavor decay in which the muon is misidentified as being isolated from other activity.

Corrections accounting for differences between data and simulated events are applied to the simulated events. The

corrections are derived from control data samples and applied to object identification efficiencies, trigger efficiencies, the primary vertex position and the transverse momentum spectrum of Z bosons. The correction factors are typically a few percent. After applying all corrections, the yields for signal and each background are calculated as the product of the acceptance times efficiency determined from simulation, luminosity and predicted cross sections.

The initial analysis step is selection of events recorded by at least one trigger from a set of single muon triggers (for data taken before the summer of 2006) or by at least one trigger from a set of single muon, and for the first time, muon plus hadronic tau triggers (for data taken after summer 2006) with the trigger efficiency for signal events of around 65%.

After making the trigger requirements a background-dominated pre-tag sample is selected by requiring a reconstructed production point for the event with at least three tracks, exactly one reconstructed hadronic tau, exactly one isolated muon, and at least one jet. This analysis requires the tau candidates to satisfy $E_T > 10$ GeV, $p_T^\tau > 7(5)$ GeV and $NN > 0.9$ for type 1(2) taus, $E_T > 10$ GeV, and $E_T > 15$ GeV, $p_T^\tau > 10$ GeV and $NN > 0.95$ for type 3 taus. Here E_T is the transverse energy of the tau measured in the calorimeter, p_T^τ is the transverse momentum sum of the associated track(s). The muon must satisfy $p_T^\mu > 12$ GeV, $|\eta| < 2.0$. It is also required to be isolated from activity in the tracker and calorimeter [17]. Selected jets have $E_T > 15$ GeV, $|\eta| < 2.5$. The tau, the muon and jets must all be consistent with arising from the same primary vertex and be separated from each other by $\Delta R > 0.5$. In addition, the muon and tau are required to have opposite charge, and the μ, \cancel{E}_T mass variable $M \equiv \sqrt{2E_T E_\mu^2 / p_T^\mu (1 - \cos(\Delta\varphi))}$ must satisfy $M < 80, 80,$ and 60 GeV for events with taus of type 1, 2 and 3 respectively. Here E_μ is the energy of the muon, and $\Delta\varphi$ is the opening angle between the \cancel{E}_T and muon in the plane transverse to the beam.

A more restrictive b -tag subsample with improved signal to background ratio is defined by demanding that at least one jet in each event is consistent with b quark production [9]. This b jet selection has a signal efficiency for this analysis of roughly 35% and a light-jet misidentification rate of roughly 0.5%.

All backgrounds except MJ are derived from simulated events as described earlier. The MJ background is derived from control data samples. A parent MJ-enriched control sample is created by requiring a muon, tau, and jet as above, but with the muon isolation requirement removed and with a lower quality ($0.3 \leq NN \leq 0.9$) tau selected. This is then used to create a b -tag subsample which requires at least one of the jets to be identified as a b jet with the same b jet selection as in the b -tag sample above. The residual contributions from SM backgrounds are subtracted from the parent and b -tag MJ control samples using simulated events.

To determine the MJ contribution in the pre-tag stage described above, a data sample is used that has the same selection as the pre-tag stage except that the leptons' charges have the same sign. This same-sign (SS) sample is dominated by MJ events. After making a subtraction of other SM background processes which contribute to this sample, the number of MJ events in the opposite-sign (OS) signal region is computed by multiplying the SS sample by the OS/SS ratio determined in a control sample selected by requiring a non-isolated muon. The OS/SS ratio is 1.05 ± 0.02 .

For the b -tag analysis stage, statistical limitations require a different approach for the MJ background than for the pre-tag stage. For the b -tag stage, two methods are used. For the first method, the per jet probability P_{tag} that a jet in the SS MJ control subsample would be identified as b a jet is determined as a function of jet p_T . P_{tag} is then convoluted with the jets in the SS pre-tag sample to determine the yield in the b -tag sample. For the second method, the MJ background is determined by multiplying the b -tag MJ control sample yield by two factors: (1) the probability that the nonisolated muon would be identified as isolated, and (2) the ratio of good tau to low-quality tau events determined in a separate control sample. The final MJ contribution in the b -tag stage is determined using the shape from the pre-tag sample with the normalization equal to the average of the two b -tag methods. We include the normalization difference between the two methods in the systematic error on the MJ contribution.

The signal to background ratio is further improved using multivariate techniques. Two separate methods are used, one to address the $t\bar{t}$ background and one to address the MJ background. For the $t\bar{t}$ background, a neural network (NNTOP) is constructed using $H_T \equiv \sum_{jets} E_T$, $E_{TOT} \equiv \sum_{jets} E + E_\tau + E_\mu$, the number of jets and $\Delta\varphi(\mu, \tau)$ as inputs. For the MJ background, a simple joint likelihood discriminant (LLMJ) is constructed using p_T^μ , p_T^τ , $\Delta R(\mu, \tau)$, $M_{\mu\tau}$ and $M_{\mu\tau\nu}$. Here $M_{\mu\tau}$ denotes the invariant mass of the muon and tau, and $M_{\mu\tau\nu}$ is the invariant mass computed from the muon, tau, and \cancel{E}_T momentum vectors. A likelihood is used for the MJ background instead of a method which uses variable correlations, for example, a NN, because of the limited statistics available in the MJ control samples. The final analysis sample is defined by selecting rectangular regions in the NNTOP versus LLMJ plane. The regions are dependent on tau type and Higgs mass and are determined by optimizing the search sensitivity using simulated events. The signal to background improves by a factor of two when applying these requirements.

Table I shows the predicted background and observed data yields for three stages in the analysis. The first column is for the pre-tag stage. The second is the b -tagged stage, and the third is after all requirements have been applied. Between 5% and 10% of $\phi \rightarrow \mu\tau_h$ decays are selected depending on m_ϕ .

Systematic uncertainties arise from a variety of sources. Most are evaluated using comparisons between data control samples and predictions from simulation. The uncertainties are divided into two categories: (1) those which affect

	Pre-Tag	b -tagged	Final
$t\bar{t}$	66 ± 1.3	39.6 ± 0.8	5.2 ± 0.3
Multijet	549 ± 26	38.5 ± 2.3	17.1 ± 1.3
$Z \rightarrow \tau\tau + \text{jets}$	1241 ± 8	18.8 ± 0.3	13.2 ± 0.2
Other Bkg	267 ± 6	5.1 ± 0.1	2.7 ± 0.1
Total Bkg	2123 ± 28	102 ± 2.4	38.2 ± 1.4
Data	2077	112	52
Signal	33.9 ± 0.7	11.2 ± 0.1	9.7 ± 0.1

TABLE I: Predicted background yield, observed data yield and predicted signal yield and their statistical uncertainties at three stages of the analysis. The signal yields are calculated assuming $\tan\beta = 40$ and a Higgs mass of $120 \text{ GeV}/c^2$ for the m_h^{max} and $\mu < 0$ scenario.

only normalization, and (2) those which also affect the shape of distributions. The sources include the jet energy calibration (2%-4%), b -tagging (3%-5%), trigger (3%-5%), luminosity (6.1%), muon identification efficiency (4.5%), tau identification (5%, 4%, 8%), tau energy calibration (3%), MJ background (25%, 10%, 10%), the $t\bar{t}$ cross section (11%), diboson cross sections (6%), $Z+(u,d,s,c)$ rate (+2%, -5%) and the $W + b$ and $Z + b$ cross sections (30%). For sources with three values, the values correspond to tau types 1, 2 and 3 respectively.

After making the final selection, the discriminant D is formed from the product of the NNTOP and LLMJ variables, $D = \text{LLMJ} \times \text{NNTOP}$. The resulting distributions for the predicted background, signal and data are shown in Fig. 1. This distribution is used as input to a significance calculation using a modified frequentist approach with a Poisson log-likelihood ratio test statistic [18]. In the absence of a significant signal we set 95% confidence level limits on the presence of neutral Higgs bosons in our data sample. The cross section limits are shown in Fig. 1 as a function of Higgs boson mass. These are translated into the $\tan\beta$ versus M_A plane giving the excluded region shown in Fig. 1. The signal cross sections and branching fractions are computed using FEYNHIGGS [19]. Instabilities in the theoretical calculation for $\tan\beta > 100$ limit the usable mass range in the translation into the $(\tan\beta, M_A)$ plane.

In summary, this Letter reports a search for production of Higgs bosons in association with a b quark using eight times more data than previous results for this channel. The data are consistent with predictions from known physics sources and limits are set in the SUSY parameter space. These cross section limits are a factor of three improvement over previous results.

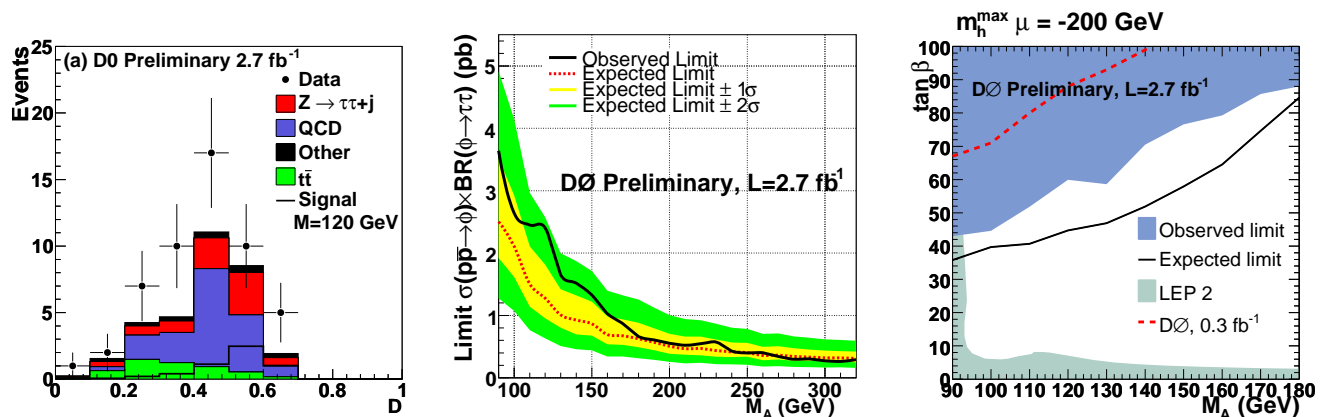


FIG. 1: (a) The distribution of the final discriminant variable, $D = \text{NNTOP} \times \text{LLMJ}$. The figure includes all tau types. (b) The cross-section limit as a function of Higgs boson mass. (c) The region in the $\tan\beta$ versus M_A plane excluded by this analysis and LEP2 searches.

-
- [1] H. P. Nilles, Phys Rep. **110**, 1 (1984); H. E. Haber and G. L. Kane, Phys. Rep. **117**, 75 (1985).
[2] V.M. Abazov *et al.* (D0 Collaboration), Phys. Rev. Lett. **102**, 051804 (2009).
[3] V.M. Abazov *et al.* (D0 Collaboration), Phys. Rev. Lett. **101**, 071804 (2008).
[4] A. Abulencia *et al.*, (CDF Collaboration), Phys. Rev. Lett. **96**, 011802 (2006).

- [5] V.M. Abazov *et al.* (D0 Collaboration), Phys. Rev. Lett, **101**, 221802 (2008).
- [6] T. Affolder *et al.*, (CDF Collaboration), Phys. Rev. Lett. **86**, 4472 (2001).
- [7] V.M. Abazov *et al.* (D0 Collaboration), Nucl. Instrum. Methods in Phys. Res. A **565**, 463 (2006).
- [8] G. Blazey *et al.*, arXiv:hep-ex/0005012 (2000).
- [9] T. Scanlon, Ph.D. Dissertation, Imperial College, FERMILAB-THESIS-2006-43 (2006).
- [10] V.M. Abazov *et al.* (D0 Collaboration), Phys. Lett. B **670**, 292 (2009).
- [11] T. Sjöstrand *et al.*, Comput. Phys. Commun. **135**, 238 (2001). Version 6.409.
- [12] J. Pumplin *et al.*, JHEP **0207** 012 (2002) and D. Stump *et al.*, JHEP **0310** 046 (2003). Version 6L1.
- [13] Z. Was, Nucl. Phys. B - Proc. Suppl. **98**, 96 (2001). Version 2.5.04.
- [14] D.J. Lange, Nucl. Instrum. Methods in Phys. Res. A **462**, 152 (2001). Version 9.39.
- [15] R. Brun and F. Carminati, CERN Program Library Long Writeup W5013, 1993 (unpublished). Version 3.21.
- [16] M.L. Mangano, M. Moretti, F. Piccinini, R. Pittau, and A. Polosa, J. High Energy Phys. **07**, 001 (2003). Version 2.11.
- [17] V.M. Abazov *et al.* (D0 Collaboration), Phys. Rev. Lett. **93**, 141801 (2004).
- [18] W. Fisher, FERMILAB-TM-2386-E (2007).
- [19] M. Frank, T. Hahn, S. Heinemeyer, W. Hollik, H. Rzehak, and G. Weiglein, JHEP 0702, 47 (2007). Version 2.65; G. Degrossi, S. Heinemeyer, W. Hollik, P. Slavich, G. Weiglein, Eur.Phys.J. C **28**, 133 (2003); S. Heinemeyer, W. Hollik, G. Weiglein, Eur.Phys.J. C **9**, 343 (1999); S. Heinemeyer, W. Hollik, G. Weiglein, Comput.Phys.Commun. **124**, 76 (2000).